

**Interaction of hexadecylbetainate chloride with biological relevant lipids**

Journal:	<i>Langmuir</i>
Manuscript ID:	la-2011-040328.R5
Manuscript Type:	Article
Date Submitted by the Author:	n/a
Complete List of Authors:	Nsimba Zakanda, Francis; University of Liege, Gembloux Agro-Bio Tech - Unité de Chimie biologique industrielle Lins, Laurence; University of Liege, Gembloux Agro-Bio Tech - Centre de Biophysique Moléculaire Numérique Nott, Katherine; University of Liege, Gembloux Agro-Bio Tech - Unité de Chimie biologique industrielle - Unité de Chimie générale et organique Paquot, Michel; University of Liege, Gembloux Agro-Bio Tech - Unité de Chimie biologique industrielle Mvumbi Lelo, Georges; Université de Kinshasa- Faculté de Médecine, Département des Sciences de Base - Service de Biochimie Deleu, Magali; University of Liege, Gembloux Agro-Bio Tech - Unité de Chimie biologique industrielle

SCHOLARONE™  
Manuscripts

## Interaction of hexadecylbetainate chloride with biological relevant lipids

F. Nsimba Zakanda<sup>a,d</sup>, L. Lins<sup>b</sup>, K. Nott<sup>a,c</sup>, M. Paquot<sup>a</sup>, G. Mvumbi Lelo<sup>d</sup> and M. Deleu<sup>a\*</sup>

<sup>a</sup> *Unité de Chimie Biologique Industrielle*, <sup>b</sup> *Centre de Biophysique Moléculaire Numérique*,  
<sup>c</sup> *Unité de Chimie Générale et Organique, Gembloux Agro-Bio Tech - University of Liege*,  
*Passage des Déportés 2, 5030 Gembloux, Belgium*

<sup>d</sup> *Service de Biochimie, Département des Sciences de Base, Faculté de Médecine, Université  
de Kinshasa B.P.127 Kinshasa XI, R.D. Congo*

\*corresponding author : [magali.deleu@ulg.ac.be](mailto:magali.deleu@ulg.ac.be) – Phone: +32 81 62 22 32 – Fax: +32

81 62 22 31

### Abstract

The present work investigates the interaction of hexadecylbetainate chloride (C<sub>16</sub>BC), a glycine betaine-based ester with palmitoyl-oleoyl-phosphatidylcholine (POPC), sphingomyelin (SM) and cholesterol (CHOL), three biological relevant lipids present in the outer leaflet of the mammalian plasma membrane. The binding affinity and the mixing behavior between the lipids and C<sub>16</sub>BC are discussed based on experimental (isothermal titration calorimetry (ITC), Langmuir film balance), and molecular modeling studies.

The results show that the interaction between C<sub>16</sub>BC and each lipid is thermodynamically favorable and does not affect the integrity of the lipid vesicles. The primary adsorption of C<sub>16</sub>BC into the lipid film is mainly governed by a hydrophobic effect. Once C<sub>16</sub>BC is inserted in the lipid film, the polar component of the interaction energy between C<sub>16</sub>BC and

1  
2  
3 the lipid becomes predominant. Presence of CHOL increases the affinity of C<sub>16</sub>BC for  
4 membrane. This result can be explained by the optimal matching between C<sub>16</sub>BC and CHOL  
5 within the film rather by a change of membrane fluidity due to the presence of CHOL. The  
6 interaction between C<sub>16</sub>BC and SM is also favorable and gives rise to highly stable  
7 monolayers probably due to hydrogen bonds between their hydrophilic groups. The  
8 interaction of C<sub>16</sub>BC with POPC is less favorable but does not destabilize the mixed  
9 monolayer from a thermodynamic point of view. Interestingly, for all the monolayers  
10 investigated, the exclusion surface pressures are above the presumed lateral pressure of the  
11 plasma membranes suggesting that C<sub>16</sub>BC would be able to penetrate into mammalian  
12 plasma membranes *in vivo*. These results may serve as a useful basis in understanding the  
13 interaction of C<sub>16</sub>BC with real membranes.  
14  
15  
16  
17  
18  
19  
20  
21  
22  
23  
24  
25  
26  
27  
28  
29  
30

31 Keywords: Cationic surfactant, glycine betaine-based ester, membrane model, bilayer,  
32 penetration, isothermal titration calorimetry, Langmuir monolayer, computational approach  
33  
34  
35  
36  
37  
38  
39  
40  
41  
42  
43  
44  
45  
46  
47  
48  
49  
50  
51  
52  
53  
54  
55  
56  
57  
58  
59  
60

## 1. Introduction

Glycine betaine (N,N,N-trimethylglycine) also called betaine is present in various plants, animals and microorganisms. Recently, a review of the synthesis methods and potential applications of glycine betaine derivatives has been published.<sup>1</sup> Betaine can be used to form the hydrophilic part of green surfactants and several surfactants including esters (alkylbetainates chlorides – C<sub>n</sub>BC) are based on this molecule.<sup>2-6</sup> These compounds are generally referred to as “mild to the skin”<sup>7</sup> and are used to improve the dermatological properties of other surfactants (e.g., alkylbetaines decrease the skin irritation of anionic compounds). From the point of view of practical applications, the study of the surface properties of these compounds is of great importance. In our previous paper<sup>8</sup>, it was found that hexadecylbetainate chloride (C<sub>16</sub>BC) forms a stable monolayer at the air-water interface under all the experimental conditions tested (pH, temperatures, ionic strengths, presence of sodium salts of monovalent or divalent anions).

Surfactants used in personal care products can cause side-effects such as cell membrane damage. Basic studies of surfactant interaction with membranes are thus of great relevance for application purposes, but also for fundamental purposes as membrane-perturbing surfactants are commonly used to lyse cells to study their contents as well as to solubilize their membrane proteins.<sup>9</sup> Considerable research is currently carried out on surfactant-lipid combinations which can be used as drug delivery systems for poorly soluble therapeutic agents.<sup>10</sup> Since C<sub>n</sub>BC are a novel class of green surface-active agents potentially useful for the formulation of a wide range of products,<sup>1</sup> in particular for the cosmetic and pharmaceutical fields, a basic physico-chemical study of their interaction with mammalian plasma membrane is required. Due to the complexity of biological membranes, interactions

1  
2  
3 with major lipid components have been examined individually as a first approach. Bilayers  
4 and monolayers of palmitoyl-oleoyl-phosphatidylcholine (POPC), sphingomyelin (SM) and  
5 cholesterol (CHOL) have been chosen as simple models. These lipids are representative of  
6 the three main types of lipids composing the outer leaflet of the mammalian plasma  
7 membrane: phospholipids, shingolipids and CHOL.<sup>11</sup>

8  
9  
10 In a recent paper<sup>8</sup>, we have suggested that primary interaction between  $C_nBC$  and lipid  
11 monolayers is mainly governed by electrostatic forces. Hydrophobic effect can also play a  
12 role when electrostatic interactions cannot occur (in the case of uncharged lipids).

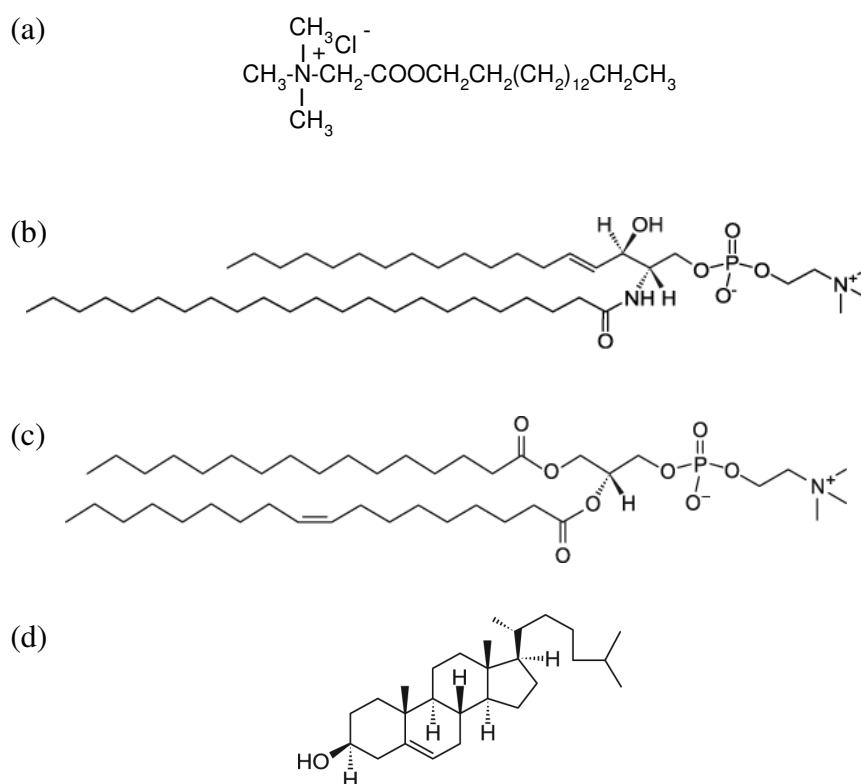
13  
14  
15 In the current work, the interaction of hexadecylbetainate chloride ( $C_{16}BC$ ) with three types  
16 of lipids (POPC, SM, CHOL) in conditions similar to biological ones (pH and ionic  
17 strength) is thoroughly examined. The isothermal titration calorimetry (ITC) technique,  
18 which measures the heat flow associated with the binding between two entities,<sup>12,13</sup> is used  
19 to obtain information about the thermodynamics of  $C_{16}BC$  binding to liposomes. Single lipid  
20 monolayer models are then used to analyze, by a simple thermodynamic approach, the  
21 mixing behavior (miscibility and stability) and the molecular interaction between each lipid  
22 and  $C_{16}BC$ . A computational analysis is also performed in order to gain further insight into  
23 the interaction at the molecular level. The results will provide some basic information about  
24 the interaction of  $C_{16}BC$  surfactant with each of the major components of the mammalian  
25 cell membrane individually or with membrane domains that might be highly enriched in a  
26 single component.

27  
28  
29  
30  
31  
32  
33  
34  
35  
36  
37  
38  
39  
40  
41  
42  
43  
44  
45  
46  
47  
48  
49  
50  
51  
52  
53  
54  
55  
56  
57  
58  
59  
60

## 2. Experimental

### 2.1. Materials

Hexadecylbetainate chloride ( $C_{16}BC$ ) (Figure 1) was synthesized in our laboratory<sup>14</sup>. Briefly, betainyl chloride was formed by adding thionyl chloride dropwise to a stirred solution of glycine betaine which was then mixed for ~ 2 hours.  $C_{16}BC$  was obtained by the acylation of 1-hexadecanol by betainyl chloride. The molecule's structure was confirmed by Infrared Spectroscopy (IR) and Mass Spectrometry (MS). A typical IR spectrum of betainyl chloride displays bands at 2960, 2870  $cm^{-1}$  ( $CH_3$ , C-H stretching), 2925, 2850  $cm^{-1}$  ( $CH_2$ , C-H stretching), 1800  $cm^{-1}$  (C=O stretching), 675  $cm^{-1}$  (C-Cl stretching). IR spectra of  $C_{16}BC$  displays bands at 2959  $cm^{-1}$  (C-H, stretching), 1751  $cm^{-1}$  (C=O stretching), 1478  $cm^{-1}$  (C-H bending), 1206  $cm^{-1}$  (C-O, stretching). Electrospray ionisation mass spectrum gives the signal of the  $[M]^+$  ion at  $m/z = 342.4$ . SM, POPC and CHOL (Figure 1) were purchased from Avanti Polar Lipids (Alabaster, AL) (99% purity). The subphase used in this work was a phosphate-buffered saline (PBS) consisting of  $NaH_2PO_4 \cdot H_2O/Na_2HPO_4/NaCl$  20/20/150 mM adjusted to pH 7.4 with NaOH. The solvents (chloroform and methanol) of analytical grade were obtained from Sigma-Aldrich (St. Louis, MO). Reagents and solvents were used as received.



32 Figure 1: Chemical structure of (a) the hexadecylbetainate chloride (C<sub>16</sub>BC) and of the three  
33 model lipids selected: (b) Sphingomyelin (SM), (c) palmitoyl-oleoyl-phosphatidylcholine  
34 (POPC), and (d) cholesterol (CHOL).  
35  
36  
37  
38  
39  
40

## 41 2.2. Methods

### 42 *Preparation of lipid vesicles*

43  
44  
45  
46  
47  
48 Large unilamellar vesicles (LUVs) were used in our experiments to study the interaction of  
49 C<sub>16</sub>BC with lipid bilayers. The vesicles were prepared using the lipid hydration technique.  
50  
51 As CHOL is unable to form bilayers<sup>15</sup> and stable LUVs, the interaction of C<sub>16</sub>BC with this  
52 lipid was studied thanks to vesicles prepared with a mixture of SM/CHOL (50:50 mol%).  
53  
54 Pure POPC, SM or SM/CHOL was dissolved in chloroform/methanol (2:1 v/v), and  
55  
56 introduced into a 10 mL round-bottom flask. A thin lipid film was obtained by removing the  
57  
58  
59  
60

1  
2  
3 solvents under vacuum with a rotary evaporator. The organic solvent traces were removed  
4  
5 by placing the flasks in a dessiccator under vacuum for 16 hours. The dried thin lipid film  
6  
7 obtained was hydrated with PBS buffer for 1 h at 30°C for POPC and 60°C for SM and  
8  
9 SM/CHOL, and shaken at 10 min intervals. Spontaneously formed multilamellar vesicles  
10  
11 (MLVs) were freeze-thawed five times with liquid nitrogen and warm water (30 or 60°C).  
12  
13 The dispersion was finally extruded fifteen times through 100-nm polycarbonate filters  
14  
15 using a Lipex Biomembranes (Vancouver, BC) extruder to obtain LUVs.  
16  
17  
18  
19  
20  
21  
22  
23

#### 24 *Isothermal Titration Calorimetry (ITC)*

25  
26 ITC measurements were performed by using a VP-ITC (MicroCal, Northampton, MA). All  
27  
28 solutions were thoroughly degassed before use by stirring under vacuum or by  
29  
30 ultrasonication. The sample cell (1.4565 mL) was loaded with PBS buffer pH 7.4 (blank) or  
31  
32 C<sub>16</sub>BC solution (30 μM) and the reference cell was filled with the PBS buffer. Titration was  
33  
34 carried out at 25°C using a 300 μL syringe filled with LUV suspension prepared in PBS pH  
35  
36 7.4. The solution in the sample cell was stirred at 305 rpm during the experiments. A  
37  
38 titration experiment consisted of consecutive injections of 5 μL LUV suspension. Each  
39  
40 injection took 10 s and a delay of 200 s was applied between each successive injection to  
41  
42 allow steady state to be attained. The effective heats were determined by subtracting the  
43  
44 values obtained for the blanks from the observed heats. Data were processed using the  
45  
46 software provided by the manufacturer (ORIGIN 7 – Originlab, Northampton, USA).  
47  
48  
49  
50  
51  
52  
53

#### 54 *Determination of the thermodynamic parameters of the C<sub>16</sub>BC binding to the lipid bilayers*

55  
56 The ITC data were treated with the cumulative model described by Heerklotz and Seelig<sup>16</sup>  
57  
58 and by Razafindralambo *et al.*<sup>17</sup> according to the following equation:  
59  
60



$$\sum_{k=1}^i \delta h_k = \Delta H_D^{w \rightarrow b} V_{cell} C_D^0 \frac{K C_L^0}{1 + K C_L^0} \quad \text{Eq 1.}$$

where  $\delta h_k$  is the heat produced following each injection (corresponds to the area of each peak on the heat flow = f(time) plot),  $\Delta H_D^{w \rightarrow b}$  is the molar enthalpy change corresponding to the transfer of C<sub>16</sub>BC from the aqueous phase (w) to the bilayer membrane (b),  $V_{cell}$  is the volume of the calorimeter sample cell (1.4565 ml),  $C_D^0$  and  $C_L^0$  are the concentrations of C<sub>16</sub>BC and of lipid in the calorimeter sample cell, respectively, and K is the binding constant.

$K$  and  $\Delta H_D^{w \rightarrow b}$  can be evaluated simultaneously by a fit of the measured cumulative heat as a function of  $C_L^0$ .

The corresponding free energy  $\Delta G_D^{w \rightarrow b}$  and the reaction entropy  $\Delta S_D^{w \rightarrow b}$  were then calculated by the standard equations:

$$\Delta G_D^{w \rightarrow b} = -RT \ln(K C_w) = \Delta H_D^{w \rightarrow b} - T \Delta S_D^{w \rightarrow b} \quad \text{Eq 2}$$

with  $R = 8.31 \text{ J} \cdot \text{mol}^{-1} \cdot \text{K}^{-1}$  and  $C_w = 55.5 \text{ M}$ .<sup>16</sup>

### *Size measurements of lipid vesicles*

Size of lipid vesicles prior to and after ITC experiments consisting of titration of C<sub>16</sub>BC solution (30  $\mu\text{M}$ ) by lipid vesicles were determined at 25°C by the dynamic light scattering technique (Delsa Nano C-Beckmann Coulter - 30 mW He-Ne laser,  $\lambda = 658 \text{ nm}$ ). Fluctuation of light scattering was measured at an angle of 160 degrees. The Non-negative least square

1  
2  
3 (NNLS) method included in the software of the instrument was used to calculate the  
4  
5 hydrodynamic diameter of the particles. Each value reported is the average of at least three  
6  
7 independent measurements.  
8  
9

### 10 11 12 *Langmuir trough technique*

13  
14 Penetration experiments of C<sub>16</sub>BC into a lipid monolayer were performed at constant area  
15  
16 (120 cm<sup>2</sup>) using an automated LB system (KSV Minitrough, KSV Instruments, Helsinki,  
17  
18 Finland). A platinum Wilhelmy plate was used to measure the surface pressure. The PBS  
19  
20 subphase temperature was maintained constant at 25 ± 1°C by circulating water through the  
21  
22 base plate on which the trough is mounted. The system was enclosed in a Plexiglas box in  
23  
24 order to minimize water evaporation and to avoid trace pollution. C<sub>16</sub>BC stock solutions  
25  
26 were prepared in PBS. Lipid monolayers were prepared at defined initial surface pressures  
27  
28 (Π<sub>i</sub> = 5, 10, 20 and 30 mN/m) by carefully spreading pure lipid solutions (SM, POPC or  
29  
30 CHOL) prepared in chloroform/methanol (2:1, v/v) onto the PBS subphase (volume ~ 89  
31  
32 mL). After waiting for stabilization of Π<sub>i</sub>, C<sub>16</sub>BC was injected into the subphase to a final  
33  
34 concentration of 1.18 μM. It is assumed that C<sub>16</sub>BC molecules exist mainly as monomers  
35  
36 within the subphase as this concentration is well below the C<sub>16</sub>BC's measured critical  
37  
38 micellar concentration (34 ± 3 μM) (data not shown). During the measurements the  
39  
40 subphase is continuously gently stirred with a magnetic bar. The difference between ΔΠ of  
41  
42 two independent sets of measurements was less than 0.5 mN/m.  
43  
44  
45  
46  
47  
48  
49

50  
51 Surface pressure (Π)–molecular area (A) compression isotherms were recorded using the  
52  
53 same LB system. C<sub>16</sub>BC and lipids (SM, POPC and CHOL) were dissolved in  
54  
55 chloroform/methanol (2:1, v/v). Pure solutions as well as binary mixtures (C<sub>16</sub>BC/SM,  
56  
57 C<sub>16</sub>BC/POPC and C<sub>16</sub>BC/CHOL with a defined composition) were prepared to a final  
58  
59 concentration of 1500 μM. A volume of 20-30 μL was spread on the PBS subphase at 25°C.  
60

1  
2  
3 After waiting for 15 min to allow for solvent evaporation and spreading of the molecules,  
4  
5 the monolayer was compressed by two barriers approaching symmetrically at a rate of 10  
6  
7 mm/min. The surface pressure was measured during the entire compression. The variation  
8  
9 coefficient of at least two independent experiments did not exceed 5%.  
10  
11

### 12 13 14 15 *Molecular modeling of C<sub>16</sub>BC/lipid interaction*

16  
17  
18 The organization and mode of interaction of the C<sub>16</sub>BC and the lipids were studied in  
19  
20 C<sub>16</sub>BC/POPC, C<sub>16</sub>BC/SM and C<sub>16</sub>BC/CHOL 1/1 molar complexes.  
21

22  
23 The modeling approach (called hypermatrix), published more than 15 years ago<sup>18</sup> and  
24  
25 upgraded<sup>19</sup>, is a “static” approach in the sense that the structure of the molecules is rigid.  
26

27  
28 This method allows to calculate the interaction between a molecule (pharmacological drug,  
29  
30 peptide, lipid analog,...) and lipids. Both molecules are first oriented at the lipid/water  
31  
32 interface using TAMMO procedure.<sup>20</sup> This allows taking implicitly the hydrophobicity of  
33  
34 the medium into account. Then, the molecule of interest (here C<sub>16</sub>BC) is fixed at the  
35  
36 interface and the molecule of lipid (POPC, SM or CHOL) is moved toward C<sub>16</sub>BC, taking  
37  
38 the position of the interface into account. By rotations and translations, more than 100.000  
39  
40 positions are tested, and the corresponding interaction energy is calculated for each position.  
41  
42

43  
44 The energy is the sum of the electrostatic, Van der Waals and hydrophobic contributions.

45  
46 The position corresponding to the lowest energy state of the complex is retained. It should  
47  
48 be noted that the calculations are not made in a free space, since the molecules are oriented  
49  
50 at the interface (and so the variation of the dielectric constant is notably taken into account)  
51  
52 and due to the fact that we calculate the hydrophobic energy using an empirical equation  
53  
54 which has been validated by comparison to experiment.<sup>21</sup> This approach implicitly takes the  
55  
56 medium into account. This method has been used for studying the interaction of numerous  
57  
58  
59  
60

1  
2  
3 molecules with lipids<sup>22,23</sup> All calculations were performed on a Linux station bi-xeon quad  
4  
5 core, using Z-ultim software.  
6  
7  
8  
9  
10  
11  
12  
13  
14  
15  
16  
17  
18  
19  
20  
21  
22  
23  
24  
25  
26  
27  
28  
29  
30  
31  
32  
33  
34  
35  
36  
37  
38  
39  
40  
41  
42  
43  
44  
45  
46  
47  
48  
49  
50  
51  
52  
53  
54  
55  
56  
57  
58  
59  
60

### 3. Results

#### 3.1. Thermodynamic analysis of the binding of C<sub>16</sub>BC to lipid bilayers

A typical isothermal titration of a C<sub>16</sub>BC aqueous solution with a LUV suspension is shown in Figure 2a. The binding of C<sub>16</sub>BC to the lipid bilayer is exothermic. The area of the peak decreases gradually with the successive LUV injections and becomes small and constant once free C<sub>16</sub>BC molecules are no longer available. The residual heat flows observed in the raw data correspond to the heat associated with the vesicle dilution in the sample cell.<sup>24</sup> Integration of the heat flow peaks in Fig. 2a gives the heats of reaction,  $\delta h_i$ . Figure 2b shows the cumulative heats ( $\sum \delta h_i$ ) as a function of the lipid concentration ( $C_L^0$ ) in the cell for the three lipids selected.

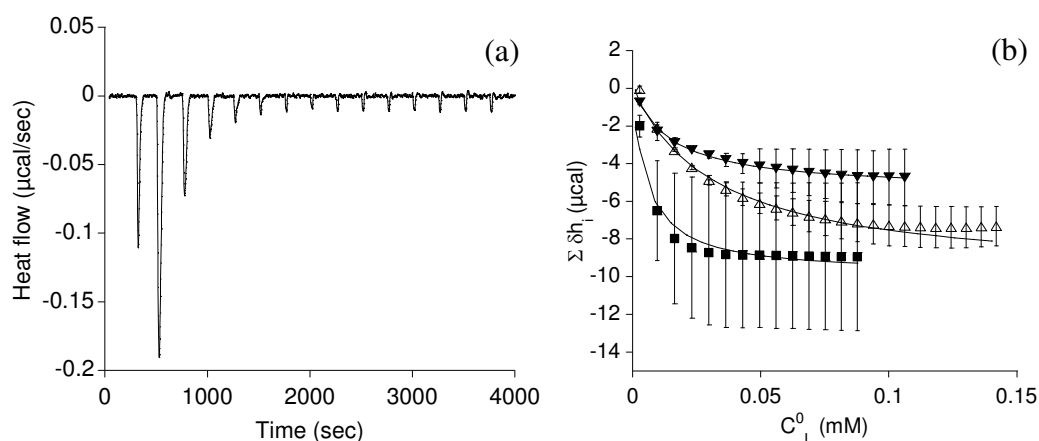
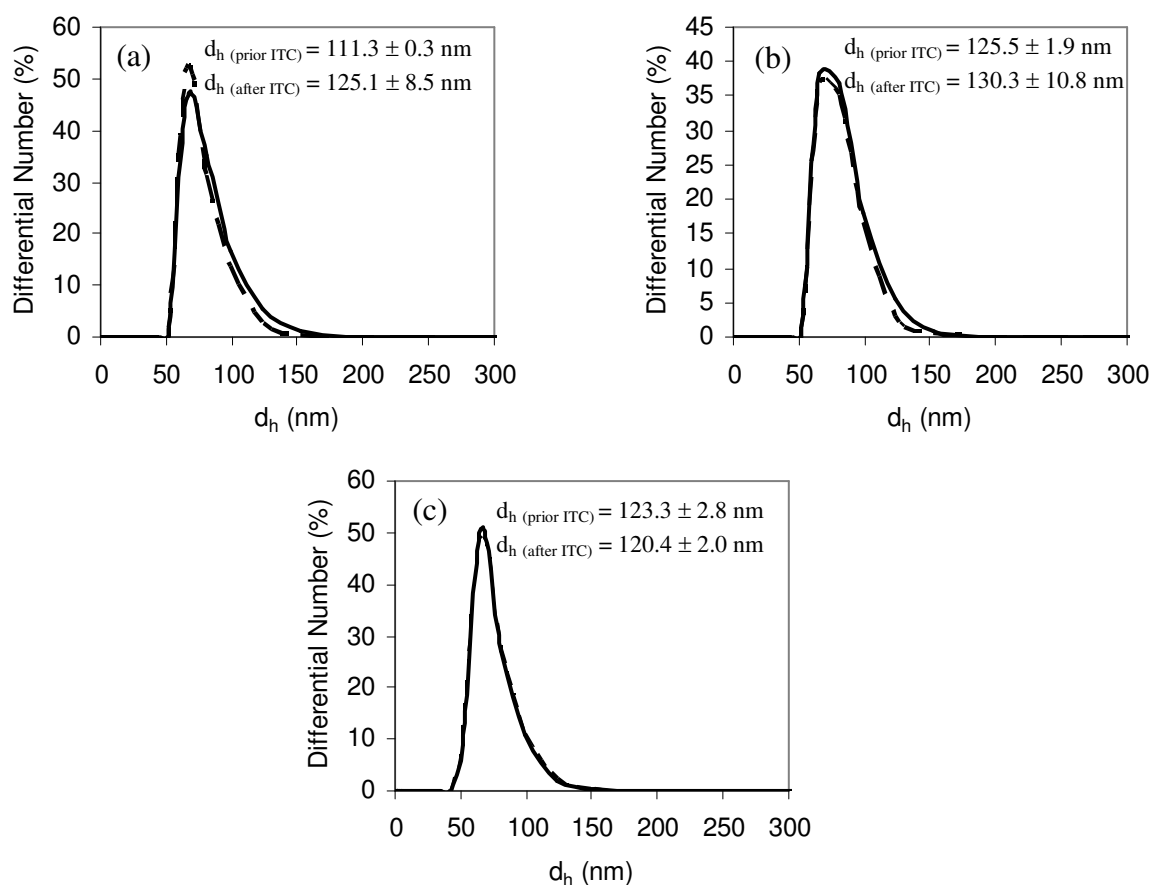


Figure 2: (a) Typical raw data of an ITC experiment. The peaks are related to the successive injections of 5  $\mu$ l of SM/CHOL LUV suspension at 1000  $\mu$ M into a 30  $\mu$ M solution of C<sub>16</sub>BC at 25°C. (b) The cumulative heats of binding ( $\sum \delta h_i$ ) as a function of the lipid concentration in the cell ( $C_L^0$ ). (■) SM/CHOL, ( $\Delta$ ) SM, ( $\blacktriangledown$ ) POPC. The solid line represents the best fit using the Eq 1. The buffer used was PBS at pH 7.4. Error bars are based on reproducibility over at least two independent measurements.

1  
2  
3  
4  
5  
6  
7  
8 The integrity of the lipid vesicles after  $C_{16}BC$  binding was checked by particle size  
9 measurements before and after ITC experiments. The mean hydrodynamic diameter of the  
10 vesicles and the size distribution are not greatly affected by the presence of  $C_{16}BC$  at  $30 \mu M$   
11 (Fig. 3). The macroscopic structure of the vesicles is thus not modified by their interaction  
12 with  $C_{16}BC$ . No population of small particles is observed suggesting that no mixed micelles  
13 are formed at this concentration of  $C_{16}BC$ .  
14  
15  
16  
17  
18  
19  
20  
21  
22



23  
24  
25  
26  
27  
28  
29  
30  
31  
32  
33  
34  
35  
36  
37  
38  
39  
40  
41  
42  
43  
44  
45  
46  
47  
48  
49  
50  
51  
52  
53 Figure 3: Particle size distribution prior to (full line) and after (dashed line) ITC experiments  
54 (a) POPC, (b) SM, (c) SM/CHOL. Inset: value of the mean hydrodynamic diameter ( $d_h$ )  
55 (average of three independent measurements).  
56  
57  
58  
59  
60

Fitting of the data of Figure 2b according to Eq. 1 and 2 gives the thermodynamic parameters listed in Table 1. It was assumed as for cetylpyridinium chloride (CPC), another positively charged ammonium detergent of similar size to C<sub>16</sub>BC,<sup>25</sup> that the C<sub>16</sub>BC flip-flop rate from the external to the internal sheet of the bilayer is fast enough to consider, in Eq. 1, the total and not only half of the lipid concentration.

Table 1: Thermodynamic parameters for the binding of C<sub>16</sub>BC to LUV with different compositions at 25°C.

Bilayer composition	K (mM <sup>-1</sup> )	$\Delta H_D^{w \rightarrow b}$ (kJ mol <sup>-1</sup> )	$T \Delta S_D^{w \rightarrow b}$ (kJ mol <sup>-1</sup> )	$\Delta G_D^{w \rightarrow b}$ (kJ mol <sup>-1</sup> )
POPC	35.3 ± 2.3	-0.72 ± 0.19	35.17 ± 2.52	-35.90 ± 2.34
SM	41.6 ± 11.0	-0.88 ± 0.18	35.32 ± 0.92	-36.20 ± 0.73
SM/CHOL	195.2 ± 13.6	-0.93 ± 0.41	39.20 ± 0.58	-40.13 ± 0.17

Regardless the composition of the vesicle, the binding reactions are spontaneous ( $\Delta G_D^{w \rightarrow b} < 0$ ), exothermic ( $\Delta H_D^{w \rightarrow b} < 0$ ), and generate a large positive change of the system entropy ( $\Delta S_D^{w \rightarrow b} > 0$ ) suggesting that the global binding is mainly entropy-driven. Tsao *et al.*<sup>26</sup> have also concluded for CPC that its insertion into bilayers is driven by an entropy gain. Marcotte *et al.*<sup>20</sup> have suggested that this entropy gain is related to the hydrophobic effect, i.e. a release of water molecules from the hydration layer of the lipid membrane and the dehydration of the C<sub>16</sub>B<sup>+</sup> ion upon binding.<sup>27,28,29</sup>

The binding constant, K, is not significantly different for the pure POPC or SM vesicles. For the SM/CHOL, K is much higher than for the pure POPC or SM vesicles. This indicates that

1  
2  
3 C<sub>16</sub>BC has a higher affinity for the SM/CHOL bilayer and that CHOL favors the binding of  
4  
5 C<sub>16</sub>BC to lipid vesicles. It is an opposite behaviour to the one reported for CPC for which  
6  
7 CHOL-containing membranes restrict its insertion.<sup>27</sup> The favorable insertion of C<sub>16</sub>BC into  
8  
9 SM/CHOL system could be accompanied by a higher release of water molecules which  
10  
11 could explain the larger entropy gain ( $\Delta S_D^{w \rightarrow b}$ ) observed in this case.  
12  
13

14  
15 At 25°C, the binary mixture SM/CHOL (50:50) is in a liquid-ordered state<sup>30,31</sup> which is an  
16  
17 intermediate situation between the solid-ordered and the liquid-disordered phases formed by  
18  
19 SM and POPC respectively. A uniform lateral distribution of SM and CHOL without  
20  
21 domain coexistence has been suggested.<sup>32</sup> Hence, the fluidity of the membrane does not  
22  
23 appear to be a critical parameter for C<sub>16</sub>BC insertion, which is in contradiction with the  
24  
25 general belief that a fluid phase is required for the incorporation of biomolecules into  
26  
27 bilayers. We suggest that distinct interactions of C<sub>16</sub>BC with the individual lipids could be at  
28  
29 the origin of the different affinities observed rather than a change of membrane fluidity.  
30  
31  
32

33  
34 To further investigate our assumption, interaction of C<sub>16</sub>BC with pure lipid monolayers of  
35  
36 single lipid was explored using the Langmuir trough technique.  
37  
38  
39  
40

### 41 3.2. C<sub>16</sub>BC penetration into pure lipid monolayers

42  
43 The ability of C<sub>16</sub>BC to interact with each lipid is studied by measuring the C<sub>16</sub>BC-induced  
44  
45 surface pressure increase ( $\Delta\Pi$ ) after the injection of C<sub>16</sub>BC beneath the pure lipid  
46  
47 monolayers performed at different initial surface pressures ( $\Pi_i$ ) (5, 10, 20 and 30 mN/m).  
48  
49  
50  
51  
52  
53  
54  
55  
56  
57  
58  
59  
60



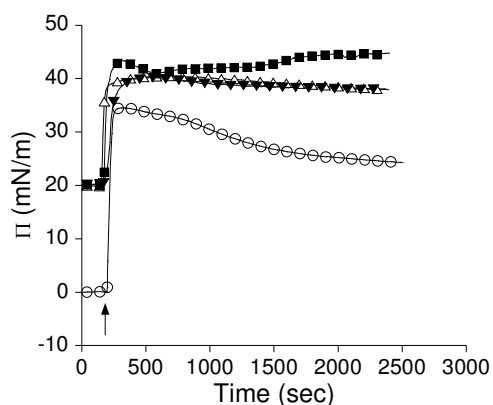


Figure 4: Typical adsorption kinetic of hexadecylbetainate chloride ( $C_{16}BC$ ) at a clean air-water interface (o) or into lipid monolayers spread at 20 mN/m: (■) CHOL, ( $\Delta$ ) SM, ( $\blacktriangledown$ ) POPC. The arrow indicates the moment at which injection occurred.  $C_{16}BC$  is injected at a final concentration of 1.18  $\mu M$  into the subphase (PBS pH 7.4; 25°C).

The adsorption of  $C_{16}BC$  at a clean air-water interface is instantaneous.  $\Pi$  attains a maximal value ( $\sim 34.5$  mN/m) and progressively decreases to reach an equilibrium ( $\sim 24.0$  mN/m) after 2000 sec (Fig. 4). The adsorption of  $C_{16}BC$  into the lipid interfaces is also instantaneous. The  $\Delta\Pi$  observed gives evidence of penetration of  $C_{16}BC$  into the lipid monolayer as explained by Marsh<sup>33</sup> and reported for other surfactants.<sup>34,35</sup> The first step of the kinetics is similar for all the lipids investigated.  $\Pi$  attains a maximal value and progressively decreases to reach the equilibrium for the SM and POPC monolayers. However, in the case of CHOL,  $\Pi$  decreases abruptly after its steep increase and then progressively rises again to reach equilibrium after  $\sim 40$  min. After its initial adsorption at

1  
2  
3 the CHOL interface, a multi-step molecular reorganization of the monolayer components  
4 likely occurs within the monolayer in order to optimize the interface arrangement.  
5  
6  
7  
8  
9

10 Fig. 5 shows the  $\Delta\Pi$  induced by  $C_{16}BC$  adsorption into the lipid monolayer as a function of  
11  $\Pi_i$ .  $\Delta\Pi$  globally decreases with  $\Pi_i$  as it is generally observed for surfactants.<sup>35</sup> In the case of  
12 SM and CHOL, a first order decrease is observed while two parts can be distinguished for  
13 the POPC curve. In this latter case,  $\Delta\Pi$  decreases slightly with  $\Pi_i$  below 10 mN/m, while it  
14 decreases more steeply above 10 mN/m.  
15  
16  
17  
18  
19  
20  
21

22 By extrapolating the curve of  $\Delta\Pi$  versus  $\Pi_i$  to the X-axis, the exclusion surface pressure of  
23 penetration ( $\Pi_e$ ) can be determined. It corresponds to the initial surface pressure above  
24 which the surfactant can no longer penetrate the monolayer. It reflects the penetration power  
25 of a surfactant. The  $\Pi_e$  are 34.2, 45.7 and 48.9 mN/m for POPC, CHOL and SM,  
26 respectively. They are above the presumed lateral pressure of the biological membranes  
27 which is estimated to be around 30 mN/m.<sup>33</sup> Molecules with  $\Pi_e$  higher than 30 mN/m are  
28 considered as potentially efficient for interaction and insertion into lipid membranes *in*  
29 *vivo*.<sup>36</sup>  
30  
31  
32  
33  
34  
35  
36  
37  
38  
39  
40

41 Moreover, the ordinates at the origin of the linear regression for the three systems  
42 investigated (30.2 , 40.8 and 31.9 mN/m for POPC, CHOL and SM respectively) are much  
43 higher than the equilibrium  $\Delta\Pi$  ( $\sim 24.0$  mN/m - Fig. 4) obtained after the adsorption of  
44  $C_{16}BC$  at the air-water (PBS, pH 7.4) interface in the absence of lipid monolayer. In PBS  
45 buffer, all the lipids tested exert thus a positive effect on  $C_{16}BC$  adsorption. In a pure water  
46 medium, it was the case for CHOL but not for POPC.<sup>14</sup>  
47  
48  
49  
50  
51  
52  
53  
54  
55  
56  
57  
58  
59  
60

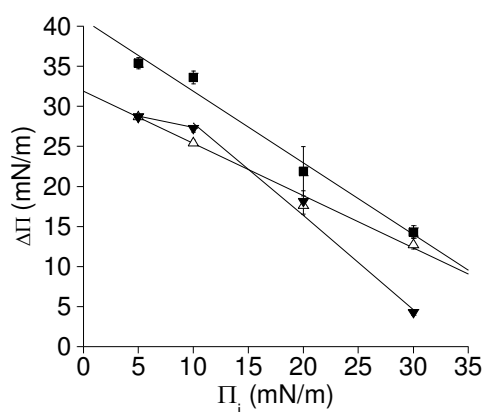


Figure 5: Surface pressure increase ( $\Delta\Pi$ ) caused by the penetration of  $C_{16}BC$  into pure monolayers of (■) CHOL, ( $\Delta$ ) SM, ( $\blacktriangledown$ ) POPC as a function of their initial surface pressure ( $\Pi_i$ ).  $C_{16}BC$  is injected beneath the lipid monolayer at a final concentration of  $1.18 \mu M$  in the PBS subphase at pH 7.4 and  $25^\circ C$ . Error bars are smaller than symbols in some cases. The solid line represents the linear fitting of the data ( $R^2 = 0.98$  and  $0.99$  for CHOL and SM respectively. For POPC, the linear fitting has been done for  $\Pi_i \geq 10$  mN/m and  $R^2 = 0.98$ ).

### 3.3. Interfacial properties of spread $C_{16}BC$ /lipid monolayers upon compression

Binary mixtures of  $C_{16}BC$  and each characteristic lipid chosen were spread at the air-water (PBS pH 7.4) interface at  $25^\circ C$  and the compression isotherms of the mixed monolayers were studied. A thermodynamic analysis is performed in order to characterize the interaction between this surfactant and the lipids.

Fig. 6a-c illustrates the  $\Pi$ -A isotherms for pure monolayers of  $C_{16}BC$ , POPC, SM and CHOL, as well as for the binary mixtures of  $C_{16}BC$  with the three lipids in different proportions. The shape of the compression isotherm recorded for  $C_{16}BC$  is typical of a condensed monolayer (Fig. 6a). The molecular area ( $A_c$ ) and the surface pressure ( $\Pi_c$ ) at the collapse are  $19.4 \pm 0.4 \text{ \AA}^2/\text{molecule}$  and  $46.2 \pm 0.5$  mN/m, respectively.  $A_c$  is higher and  $\Pi_c$

1  
2  
3 lower with the PBS subphase than with the pure water subphase used in our previous study  
4  
5 (17.3 ± 0.3 Å<sup>2</sup>/molecule and 52.3 ± 0.6 mN/m).<sup>14</sup> This is the result of the interaction between  
6  
7 the positive head groups of C<sub>16</sub>BC molecules and the subphase hydrophilic anions (H<sub>2</sub>PO<sub>4</sub><sup>-</sup>,  
8  
9 HPO<sub>4</sub><sup>2-</sup> and Cl<sup>-</sup>) which expands and slightly destabilizes the C<sub>16</sub>BC monolayer.<sup>37</sup>  
10  
11  
12  
13  
14

15 The compression isotherm recorded for POPC (Fig. 6a) is characteristic of a liquid expanded  
16  
17 monolayer with no discontinuities suggestive of phase changes, in accordance with the  
18  
19 literature.<sup>38</sup> The collapse parameters are A<sub>c</sub> = 58.5 ± 0.9 Å<sup>2</sup>/molecule and Π<sub>c</sub> = 40.8 ± 1.7  
20  
21 mN/m. The isotherm recorded for SM is also typical of liquid expanded monolayers until  
22  
23 ~25 mN/m at which a slight increase in slope is observed suggesting a more condensed state  
24  
25 for the monolayer (Fig. 6b and Supporting Information). The shape is similar to those of the  
26  
27 isotherms previously obtained.<sup>39</sup> The A<sub>c</sub> is 43.1 ± 1.5 Å<sup>2</sup>/molecule and Π<sub>c</sub> is 43.7 ± 2.1  
28  
29 mN/m. The shape of the compression isotherm for CHOL (Fig. 6c) indicates that this sterol  
30  
31 forms a highly condensed monolayer at the air–water interface. An area of 40.6 Å<sup>2</sup>/molecule  
32  
33 at 20 mN/m is in agreement with the literature.<sup>40,41,42</sup> The collapse parameters observed are  
34  
35 A<sub>c</sub> = 34.1 ± 0.8 Å<sup>2</sup>/molecule and Π<sub>c</sub> = 43.2 ± 0.1 mN/m.  
36  
37  
38  
39  
40  
41  
42  
43

44 The compression isotherms for mixed systems (C<sub>16</sub>BC/POPC, C<sub>16</sub>BC/SM and  
45  
46 C<sub>16</sub>BC/CHOL) lie between those of the pure components. Increase of the C<sub>16</sub>BC  
47  
48 concentration shifts the isotherms towards the curve of pure C<sub>16</sub>BC. The shape of the mixed  
49  
50 isotherms is not significantly influenced by the proportion of C<sub>16</sub>BC. Their Π<sub>c</sub> values are  
51  
52 between those of the pure components with the exception of the mixed C<sub>16</sub>BC/SM  
53  
54 monolayers for which Π<sub>c</sub> is much higher for all the proportions studied.  
55  
56  
57  
58  
59  
60

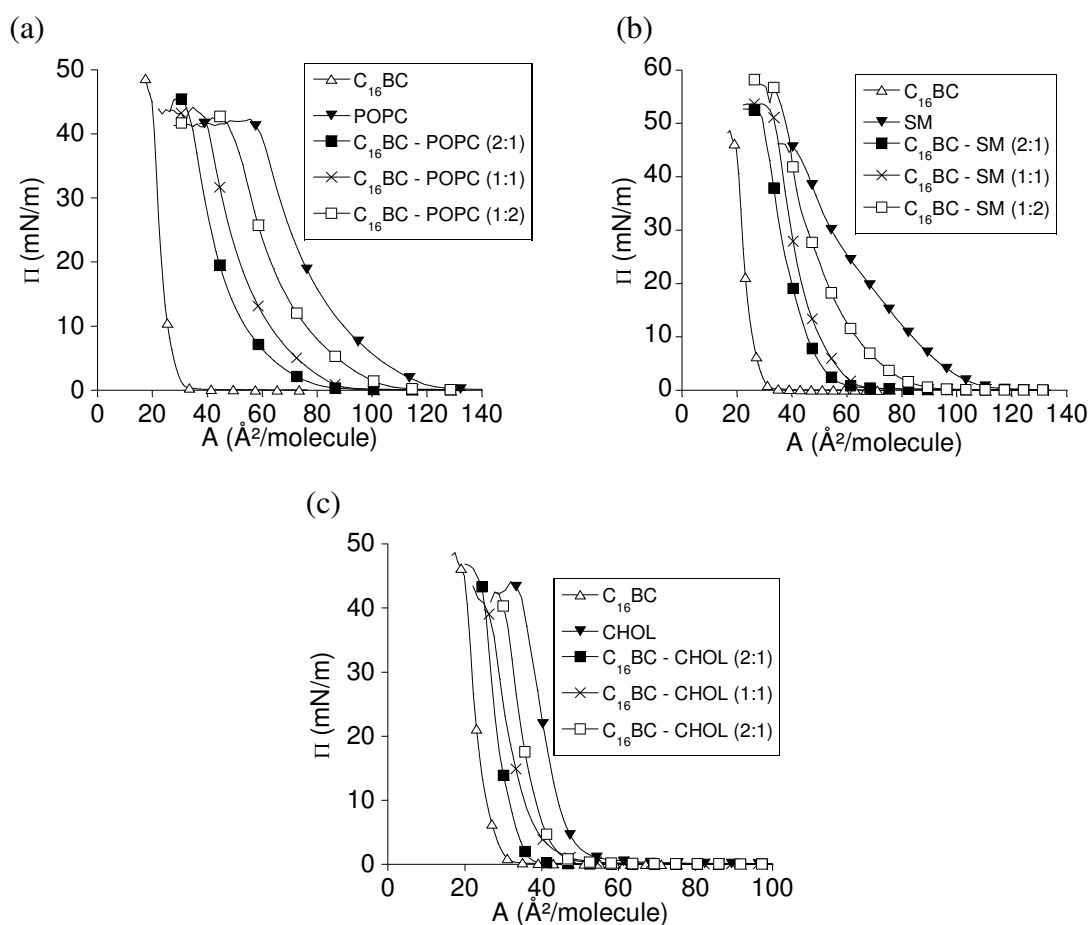


Figure 6: Surface pressure ( $\Pi$ )–molecular area ( $A$ ) isotherms for C<sub>16</sub>BC and lipid mixtures spread onto PBS subphase pH 7.4 at 25°C: C<sub>16</sub>BC/POPC (a), C<sub>16</sub>BC/SM (b) and C<sub>16</sub>BC/CHOL (c).

A simple thermodynamic analysis of compression isotherm data can give further information about the miscibility and the interaction between the components in the mixed monolayers. The plots of the mean molecular area ( $A$ ) of the mixed monolayer as a function of the C<sub>16</sub>BC molar ratio are shown in Fig. 7 for three  $\Pi$  (10, 20 and 30 mN/m). If the components of the monolayer are completely immiscible or ideally miscible, the molecular area is a linear function of the composition and follows the additivity rule given by equation

1  
2  
3 3. A deviation from ideal behavior suggests the existence of interaction between the  
4  
5 molecules and a partial miscibility.<sup>39</sup>  
6  
7

$$A_{12} = A_1 X_1 + A_2 X_2 \quad \text{Eq. 3}$$

8  
9  
10  
11  
12 where  $A_{12}$  is the mean molecular area for ideal mixing of the two components at a given  $\Pi$ ,  
13  
14  $A_1$  and  $A_2$  are the molecular areas of the respective components in their pure monolayers at  
15  
16 the same  $\Pi$  and  $X_1$  and  $X_2$  are the molar ratios of components 1 and 2 in the mixed  
17  
18 monolayers.  
19  
20  
21  
22

23  
24  
25 A small positive deviation from ideal behavior is observed for most of the  $C_{16}BC/POPC$   
26  
27 monolayers at  $\Pi \leq 20$  mN/m. In the case of SM, a negative deviation of  $A$  is observed for  
28  
29  $C_{16}BC$  molar ratio of 0.5 at 10 and 20 mN/m while no or small positive deviations are noted  
30  
31 at 30 mN/m. For these monolayers, interaction occurs between the components whereas an  
32  
33 ideal behavior is observed for the  $C_{16}BC/CHOL$  for the whole range of compositions and  $\Pi$   
34  
35 investigated. The mean molecular areas of  $C_{16}BC$  and  $CHOL$  are not influenced by the  
36  
37 presence of the other. In other words, it indicates that no interaction exists between the  
38  
39 components. In such a case, there are two possibilities for their distribution within the  
40  
41 monolayer: either the two components are completely immiscible or they are completely  
42  
43 miscible.  
44  
45  
46  
47  
48  
49  
50  
51  
52  
53  
54  
55  
56  
57  
58  
59  
60

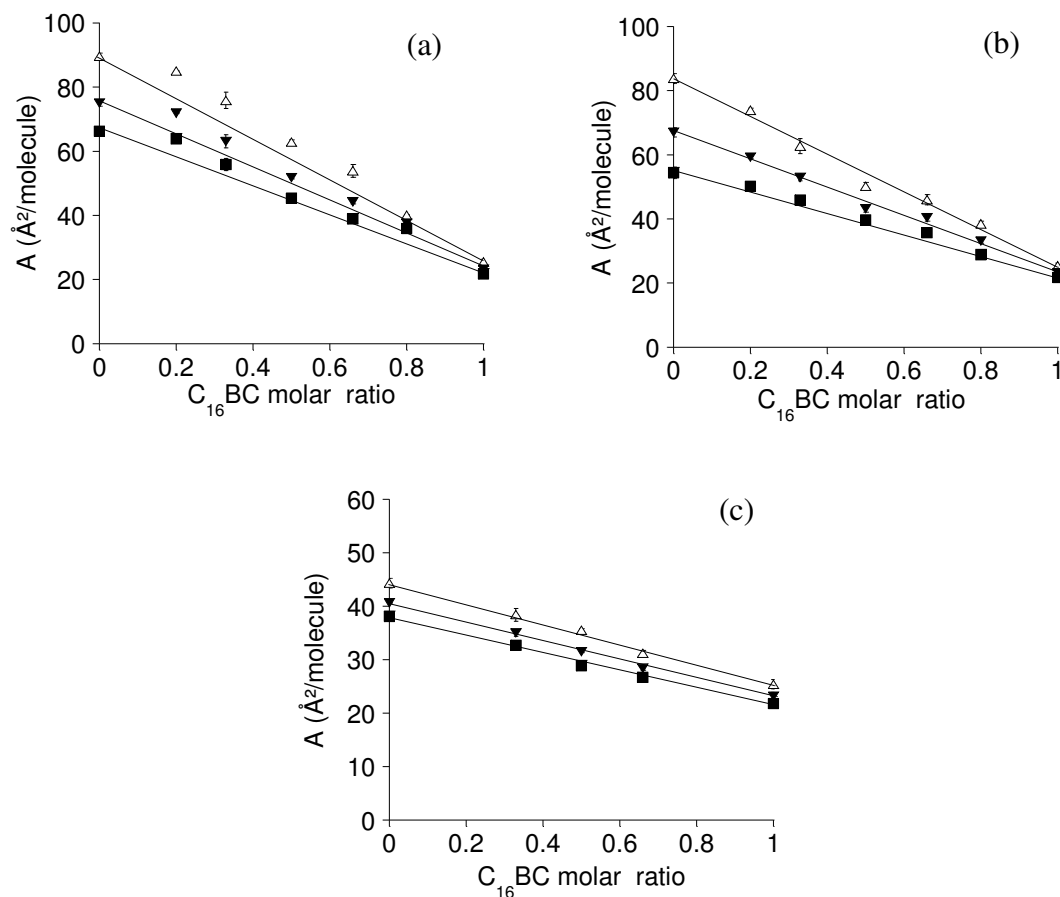


Figure 7: Mean molecular area ( $A$ ) versus composition plot for the mixtures of  $C_{16}BC$  with POPC (a), SM (b) and CHOL (c) at different  $\Pi$  ( $\Delta$ ) 10 mN/m, ( $\nabla$ ) 20 mN/m and ( $\blacksquare$ ) 30 mN/m) at 25°C. Straight lines correspond to the ideal mixing behavior (Eq. 3). In some cases, the error bars are smaller than the symbols.

A more quantitative thermodynamic analysis of the mixtures can be obtained by calculating the excess free energy of mixing  $\Delta G^{ex}$  (eq. 4) and the total free energy of mixing ( $\Delta G^M$ ) (eq. 5).<sup>43</sup>

$$\Delta G^{ex} = \int_0^{\Pi} (A_{12} - X_1 A_1 - X_2 A_2) d\Pi \quad \text{Eq. 4}$$

$$\Delta G^M = \Delta G^{ex} + \Delta G^{id} \quad \text{Eq. 5}$$

where  $\Delta G^{id}$  is the free energy for ideal mixing and is defined by equation 6.

$$\Delta G^{id} = RT(X_1 \ln X_1 + X_2 \ln X_2) \quad \text{Eq. 6}$$

where R is the universal gas constant and T, the absolute temperature.

$\Delta G^{ex}$  provides information about the possible interaction between the monolayer forming components.<sup>34</sup>

Negative values of  $\Delta G^{ex}$  indicate that the interactions between the components in the mixed monolayers are more attractive or less repulsive compared to those occurring in their respective pure monolayers. Positive values of  $\Delta G^{ex}$  suggest that the interactions are less attractive or more repulsive than those existing in the one-component monolayers.<sup>44,45,46</sup>

$\Delta G^M$  gives information about the thermodynamic stability of the mixed monolayers. A negative value indicates that the system is stable.<sup>34</sup>

$\Delta G^{ex}$  and  $\Delta G^M$  as a function of the C<sub>16</sub>BC molar ratio plots are shown in Fig. 8a-f. Globally, their absolute values are lower than those observed for similar systems such as dialkyldimethylammonium bromides-sterol<sup>44</sup>. Nevertheless, they are statistically different from ideal mixing and provide some further insight into the different affinities between C<sub>16</sub>BC and the three bilayer components. The positive values of  $\Delta G^{ex}$  obtained for most of C<sub>16</sub>BC/POPC mixed monolayers (Fig. 8a) indicate repulsive interaction between the monolayer forming components. This suggests that, at least one component forms two-dimensional aggregates at the interface.<sup>34,46</sup> C<sub>16</sub>BC/SM mixed monolayers show nil or negative  $\Delta G^{ex}$  at C<sub>16</sub>BC molar ratio  $\leq 0.5$  (Fig. 8b). This suggests that attractive interaction exists within the mixed monolayers between C<sub>16</sub>BC and SM molecules. However, positive deviations, that can be related to repulsive interactions, are observed at C<sub>16</sub>BC molar ratio = 0.66 and 0.8. No deviation is observed for the C<sub>16</sub>BC/CHOL pairs (Fig. 8c) confirming the ideal behaviour of these mixtures.



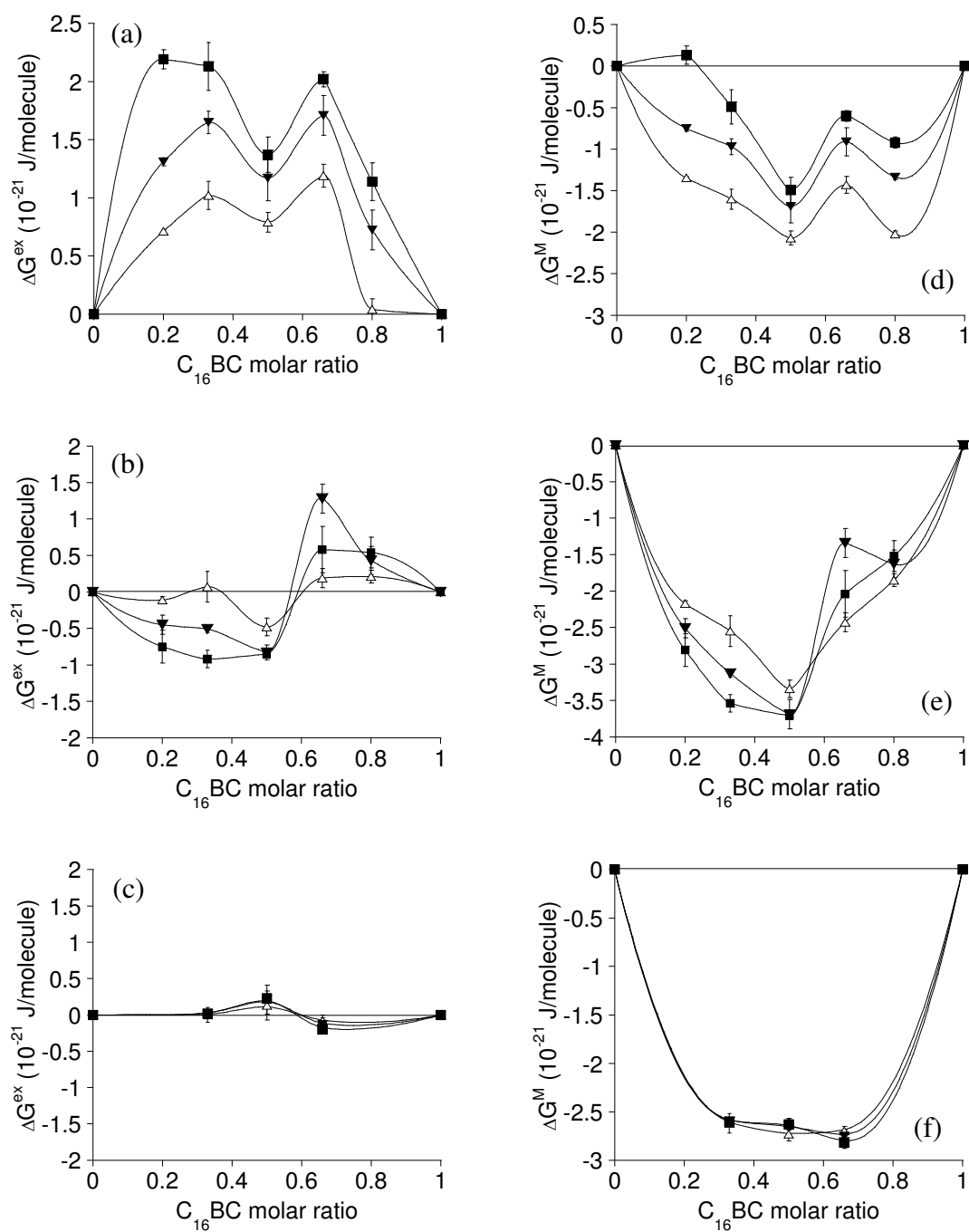


Figure 8: Excess free energy of mixing ( $\Delta G^{ex}$ ) and total free energy of mixing ( $\Delta G^M$ ) versus  $C_{16}BC$  molar ratio for the mixtures of  $C_{16}BC$  with POPC (a, d), SM (b, e) and CHOL (c, f)

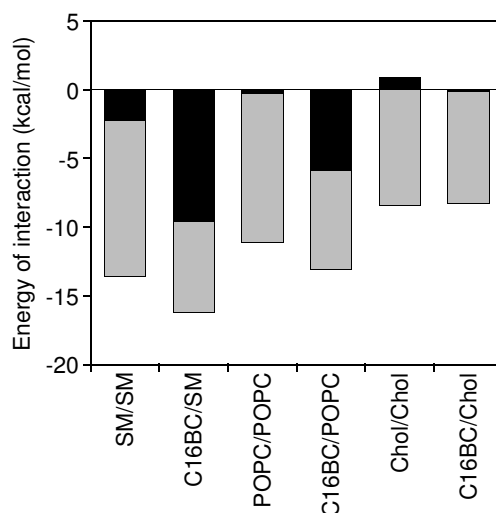
1  
2  
3 at different  $\Pi$  ( $\Delta$ ) 10 mN/m, ( $\blacktriangledown$ ) 20 mN/m) and ( $\blacksquare$ ) 30 mN/m and at 25°C. Error bars are  
4  
5 smaller than symbols in some cases.  
6  
7

8  
9  
10 The values of  $\Delta G^M$  in Fig. 8d-f are negative for most of the  $C_{16}BC/POPC$ , all the  $C_{16}BC/SM$   
11  
12 and all the  $C_{16}BC/CHOL$  mixed monolayers implying that the mixing behaviour of  $C_{16}BC$   
13  
14 and each lipid is thermodynamically favorable within the whole range of composition and  $\Pi$   
15  
16 investigated. At a given  $\Pi$ ,  $\Delta G^M$  is more negative for  $C_{16}BC/SM$  and  $C_{16}BC/CHOL$  systems  
17  
18 than for  $C_{16}BC/POPC$ . The mixed monolayers formed with SM and CHOL are more stable  
19  
20 than those with POPC. For the  $C_{16}BC/POPC$  mixed monolayers,  $\Delta G^M$  increases as  $\Pi$   
21  
22 increases, suggesting that the mixed monolayers become less stable at higher  $\Pi$ . At  $\Pi = 30$   
23  
24 mN/m,  $C_{16}BC/POPC$  (1:1) mixed monolayer is the most stable monolayer (Fig. 8d). For the  
25  
26 mixed  $C_{16}BC/SM$  monolayers, at a  $C_{16}BC$  molar ratio  $\leq 0.5$ , the stability of the mixed  
27  
28  $C_{16}BC/SM$  monolayers increases with  $\Pi$  while at  $C_{16}BC$  molar ratio = 0.66, the stability  
29  
30 decreases with increasing  $\Pi$  (Fig. 8e). The stability of  $C_{16}BC/CHOL$  is not influenced by  
31  
32  $\Pi$  (Fig. 8f).  
33  
34  
35  
36  
37  
38  
39  
40  
41

### 42 3.4. Molecular modeling

43  
44 The Hypermatrix method used for the molecular modeling is a “static” approach in the sense  
45  
46 that the structure of the molecules is rigid<sup>19</sup>. Issues that might be sensitive to the way in  
47  
48 which the chains are folded within the bilayer cannot thus be explored but this approach is  
49  
50 particularly useful for investigating the nature of the interaction of drugs and other  
51  
52 molecules with specific parts of the membrane and for estimating how the molecular area is  
53  
54 affected by the interactions in the vicinity of the hydrophobic/hydrophilic interface.  
55  
56  
57  
58  
59  
60

1  
2  
3 The calculation of the interaction energy between one molecule of SM or POPC and one  
4 molecule of C<sub>16</sub>BC (Fig. 9) shows that these associations lower the total energy, as  
5 compared to pure lipids.  
6  
7  
8  
9



10  
11  
12  
13  
14  
15  
16  
17  
18  
19  
20  
21  
22  
23  
24  
25  
26  
27  
28  
29  
30 Figure 9: Total energy of interaction between the pure lipid molecules and between each  
31 lipid and C<sub>16</sub>BC. Black and grey bars correspond to the polar and the hydrophobic  
32 contributions, respectively.  
33  
34  
35  
36  
37  
38  
39

40 The most favorable interaction is obtained with SM which is in accordance with the  $\Delta G^M$   
41 values at C<sub>16</sub>BC molar ratio = 0.5. For SM and POPC, the polar contribution increases  
42 markedly when they interact with C<sub>16</sub>BC while the energy is mainly of hydrophobic origin  
43 for pure lipid self-association. In both cases, the PO<sub>4</sub><sup>-</sup> of the lipid is close to the quaternary  
44 ammonium of C<sub>16</sub>BC (Fig. 10a and b) and can then interact electrostatically. Moreover, the  
45 ester moiety of C<sub>16</sub>BC is located at the level of the amide and the hydroxyl groups of SM  
46 (Fig. 10b). Formation of H bonds between these groups can also contribute to the polar  
47 component of the interaction energy.  
48  
49  
50  
51  
52  
53  
54  
55  
56  
57  
58  
59  
60

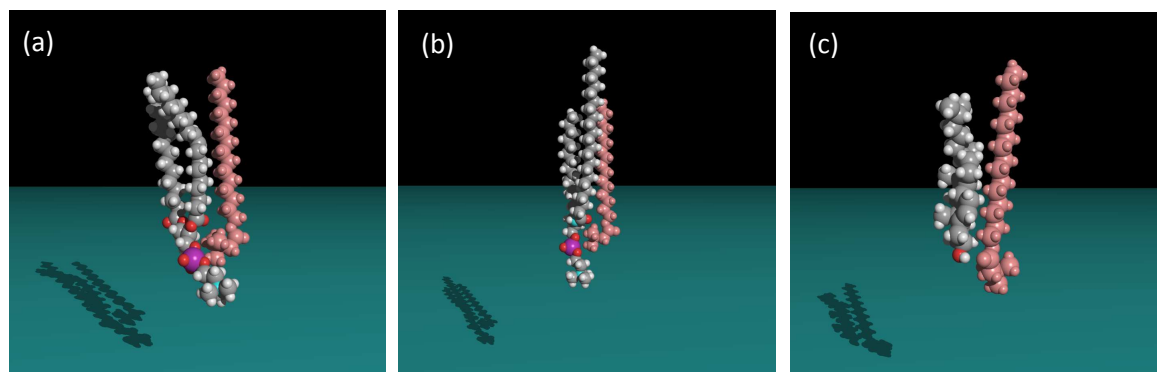


Figure 10: Molecular assembly of  $C_{16}BC$  (in pink) with (a) POPC, (b) SM and (c) CHOL at an hydrophobic/hydrophilic interface.

In the case of CHOL, the interaction energies with  $C_{16}BC$  or with itself are similar. Furthermore, the total calculated interfacial area occupied by both molecules in the assembly ( $94 \text{ \AA}^2$ ) is equal to the addition of the individual molecular areas ( $54 \text{ \AA}^2$  for CHOL and  $39 \text{ \AA}^2$  for  $C_{16}BC$ ) in accordance with our experimental results (Fig. 6c). The assembly of  $C_{16}BC$  and CHOL does not appear to disturb their self arrangement at the interface. Their fitting shown in Fig. 10c can be considered as ideal. The OH group of CHOL is at the level of the  $C_{16}BC$  ester bond, slightly decreasing the polar energy as compared to pure CHOL assembly and the sterol rings are parallel to  $C_{16}BC$  alkyl chain, generating a large hydrophobic contribution to the interaction energy, as for pure CHOL.

#### 4. General discussion and conclusion

The negative binding free energies ( $\Delta G_D^{w \rightarrow b}$  – Table 1) of C<sub>16</sub>BC for the lipid systems investigated indicate that the transfer of C<sub>16</sub>BC from the aqueous phase into lipid bilayers is thermodynamically favorable. C<sub>16</sub>BC surfactant (at a concentration near its CMC) is able to bind to lipid vesicles without compromising their integrity (Fig. 3). The increase of the surface pressure after the injection of C<sub>16</sub>BC beneath the lipid monolayers also gives evidence of C<sub>16</sub>BC penetration into all the lipid films investigated. Moreover, the exclusion pressure of C<sub>16</sub>BC for the three lipids is above the presumed surface pressure of biological membranes, suggesting that C<sub>16</sub>BC could be able to insert into *in vivo* mammalian plasma membranes containing high concentration of these three lipids.

Bilayer binding constant (K –Table 1) and monolayer equilibrium  $\Delta\Pi$  (Fig. 4) values clearly show that the insertion of C<sub>16</sub>BC is more important for the CHOL-containing films than for SM or POPC films. However, one could expect penetration to be favored into POPC as this lipid forms liquid-disordered lamellar phase<sup>30</sup> and monolayers less packed than those of CHOL or SM at a given surface pressure.<sup>47,48</sup> Our measurements indicate otherwise. It means that membrane fluidity is not the key feature to explain distinct C<sub>16</sub>BC insertion between SM/CHOL and, SM and POPC.

Higher affinity of hexadecylphosphocholine, another quaternary ammonium surfactant with a 16 carbon atoms chain, for CHOL rather than POPC has also been previously reported.<sup>49</sup>

This may be due to the fact that the CHOL sterol rings can fit nicely into the C<sub>16</sub>BC alkyl-chain region and that its hydroxyl group helps to anchor the CHOL molecule at the C<sub>16</sub>BC head–alkyl-chain interface as shown by the molecular modeling of their assembly (Fig. 10c).

This suggests an ideal miscibility, i.e. a uniform distribution, of C<sub>16</sub>BC and CHOL, and

1  
2  
3 corroborates the ideal behavior observed for the mixed C<sub>16</sub>BC/CHOL monolayers (Fig. 7).  
4  
5 However, the kinetic of their optimal mutual organization is slow as shown by the long  
6  
7 stabilizing time of  $\Delta\Pi$  observed in monolayer systems (Fig. 4). The very small value of  $\Delta G^{\text{ex}}$   
8  
9 for C<sub>16</sub>BC-CHOL monolayers seems to be inconsistent with the large  $\Delta S_D^{w \rightarrow b}$  observed for  
10  
11 the C<sub>16</sub>BC-CHOL-SM bilayer. However, both parameters do not reflect the same  
12  
13 phenomenon. In the bilayer experiments there is an adsorption and insertion stage while in  
14  
15 the monolayer experiments, both molecules are spread simultaneously at the interface and  
16  
17 no adsorption phenomenon occurs. The  $\Delta S_D^{w \rightarrow b}$  value calculated from bilayer results takes  
18  
19 into consideration the global interaction phenomenon comprising the adsorption, the  
20  
21 insertion and the rearrangement of both components due to their strictly speaking interaction  
22  
23 while the  $\Delta G^{\text{ex}}$  calculated from monolayer data is restricted to the last step.  
24  
25  
26  
27  
28  
29

30 POPC has a larger head group than CHOL and cannot pack tightly due to head-tail  
31  
32 mismatch, causing its tail group to be tilted even at high surface pressures. Moreover, the  
33  
34 presence of a cis double bond in the hydrocarbon chain of POPC prevents their close  
35  
36 packing and increases the intermolecular distance in the monolayer<sup>50</sup> as reflected in the area  
37  
38 per molecule in the one-component monolayer (Fig. 6). The steric hindrance of the POPC  
39  
40 molecule is high and insertion of C<sub>16</sub>BC molecules between POPC molecules is less  
41  
42 favorable. Similar results have been obtained for the interaction between stearic acid and  
43  
44 DOPC.<sup>51</sup>  
45  
46  
47  
48

49 SM possesses a trans double bond located at the C<sub>4</sub>-C<sub>5</sub> of its sphingosine backbone (Fig.  
50  
51 1b), and shows a tighter packing than POPC in its monolayer ( $A_c$  values from Fig. 6).<sup>52,53</sup>  
52  
53 Hydrogen bonds between the amide or the hydroxyl of the acyl chain of SM and the  
54  
55 carbonyl group of C<sub>16</sub>BC can be formed, favoring the polar interaction between the  
56  
57 molecules. Moreover, they can promote the van der Waals interactions between the alkyl  
58  
59  
60

1  
2  
3 chains of C<sub>16</sub>BC and of SM.<sup>54</sup> These interactions stabilize the monolayer as shown by their  
4  
5 negative  $\Delta G^M$  (Fig 8e) and the much higher  $\Pi_c$  for the mixed systems compared to the pure  
6  
7 ones (Fig. 6b). However, with a C<sub>16</sub>BC molar ratio > 0.5,  $\Delta G^{ex}$  (Fig 8b) becomes positive  
8  
9 and the interactions are thus more repulsive. Hydrogen bonds between the hydrophilic  
10  
11 groups can explain the more favorable C<sub>16</sub>BC interaction with the SM monolayer rather than  
12  
13 with the POPC as highlighted by the computer modeling calculation and as reflected by the  
14  
15  $\Pi_c$  determined. In bilayers, this difference is not significant. A higher flip-flop rate of C<sub>16</sub>BC  
16  
17 from the outer to the inner leaflet of the POPC bilayer could compensate this effect.  
18  
19  
20  
21  
22  
23  
24

25 In general conclusion, this study has shown that the interaction between C<sub>16</sub>BC and lipids is  
26  
27 not governed by the membrane fluidity and that the forces involved can have an origin other  
28  
29 than purely electrostatic, confirming the hypothesis developed in our previous paper.<sup>14</sup> The  
30  
31 primary insertion of C<sub>16</sub>BC into lipid vesicles is mainly governed by an hydrophobic effect.  
32  
33 Subsequently, a convenient geometrical arrangement between the lipid and C<sub>16</sub>BC involving  
34  
35 polar interaction is favorable for their association. A best arrangement between surfactin, a  
36  
37 lipopeptide, and dipalmitoyl-phosphatidyl-ethanolamine (DPPE) molecules has also been  
38  
39 shown to be at the origin of the stabilizing effect of surfactin towards DPPE monolayer.<sup>55</sup>  
40  
41  
42  
43 The optimal matching between the surfactant and a lipid for which the packing parameter is  
44  
45 not in favor of the formation of a bilayer as it is the case for CHOL, can also stabilize the  
46  
47 lamellar structure. Hydrogen bonds between the surfactant and the lipid also contribute to  
48  
49 the monolayer stabilization.  
50  
51  
52  
53  
54

55 Although this study mainly provides basic insights about the interaction of C<sub>16</sub>BC with each  
56  
57 of the major membrane components taken individually, it may serve as a useful basis for  
58  
59 understanding the interaction of C<sub>16</sub>BC with real membranes or at least, with membrane  
60

1  
2  
3 domains that might be highly enriched in a single component. It may be suggested that  
4  
5 under physiological conditions, C<sub>16</sub>BC can interact with the outer leaflet of mammalian  
6  
7 plasma membranes without compromising their stability. The presence of rafts composed by  
8  
9 SM and CHOL could be favorable to the interaction. However, it must be kept in mind that  
10  
11 the interaction of a surfactant with a real membrane might be sensitive to many properties  
12  
13 that reflect the mixing of membrane components such as average chain order, average area  
14  
15 per lipid, local surface potential, and the lateral distribution of lipid components. Further  
16  
17 investigations using ternary mixtures of the three lipids investigated as more representative  
18  
19 models of mammalian plasma membrane have to be performed to assess our hypothesis.  
20  
21 Moreover, molecular dynamic calculations taking into consideration the reorientation of the  
22  
23 molecules about the bilayer normal and the fast acyl chain conformation changes could also  
24  
25 provide additional information about the interaction of C<sub>16</sub>BC in a dynamic environment,  
26  
27 more representative of a real membrane.  
28  
29  
30  
31  
32  
33  
34  
35  
36  
37  
38  
39  
40  
41  
42  
43  
44  
45  
46  
47  
48  
49  
50  
51  
52  
53  
54  
55  
56  
57  
58  
59  
60



## Acknowledgments

The research was funded through the ARC grant, financed by the French Community of Belgium and the Belgium Technical Cooperation (BTC). M.D. and L.L. thanks the Belgian National Foundation for Scientific Research (FNRS) for their position as Research Associate and Senior Research Associate positions respectively.

## Supporting information

Enlargement of the  $\Pi$ -A isotherm of SM monolayer showing the change of slope at  $\sim 25$  mN/m.

This information is available free of charge via the Internet at <http://pubs.acs.org/>.

**References**

- (1) Nsimba Zakanda, F.; Paquot, M.; Mvumbi Lelo, G.; Deleu M. *Biotechnol. Agron. Soc. Environ.* **2010**, *14*, 737-748.
- (2) Joung, W.-D.; Han, Y.-K.; Oh, S.-G.; Yi, S.-C. *Synth. Metals*, **2001**, *117*, 181-182.
- (3) Wydro, P. *J. Colloid Interface Sci.* **2007**, *316*, 107-113.
- (4) de la Maza, A.; Parra, J.L. *J. Control. Rel.* **1995**, *37*, 33-42.
- (5) Thompson, R.A.; Allenmark, S. *J. Colloid Interface Sci.* **1992**, *148*, 241-246.
- (6) Lundberg, D.; Ljusberg-Wahren, H.; Norlin, A.; Holmberg, K. *J. Colloid Interface Sci.* **2004**, *78*, 478-487.
- (7) Mohlin, K.; Karlsson, P.; Holmberg, K. *Colloids Surfaces A.* **2006**, *274*, 200-210.
- (8) Nsimba Zakanda, F.; Laurent, P.; Paquot, M.; Mvumbi Lelo, G.; Deleu, M. *Thin Solid Films.* **2011**, *520*, 344-350.
- (9) Nararrete, R.; Serrano, R. *Biochim. Biophys. Acta.* **1983**, *728*, 403-408.
- (10) Knauf, K.; Meister, A.; Kerth, A.; Blume, A. *J. Colloid Interface Sci.* **2010**, *342*, 243-252.
- (11) Koval, M.; Pagano, R.E. *Biochim. Biophys. Acta* **1991**, *1082*, 113-125.
- (12) Andersen, K.; Westh, P.; Otzen, D. E. *Langmuir.* **2008**, *15*, 399-407.
- (13) Nielsen, A. D.; Arleth, L.; Westh, P. *Biochim. Biophys. Acta.* **2005**, *1752*, 124-132.
- (14) Nsimba Zakanda, F.; Nott, K.; Paquot, M.; Mvumbi Lelo, G.; Deleu, M. *Colloids Surf. B.* **2011**, *86*, 176-180.
- (15) de Oliveira C.A.; Machado, A.E.H.; Pessine, F.B.T. *Chem. Phys. Lipids.* **2005**, *133*, 69-78
- (16) Heerklotz, H.; Seelig, J. *Biochim. Biophys. Acta.* **2000**, *1508*, 69-85.
- (17) Razafindralambo, H.; Dufour, S.; Paquot, M.; Deleu, M. *J. Thermal Anal. Calorimetry.* **2009**, *95*, 817-821.

- 1  
2  
3 (18) Brasseur, R. ; Killian, J.A. ; De Kruijff, B. ; Ruyschaert, J.M. *Biochim. Biophys. Acta.*  
4  
5 **1987**, *903*, 11-17.  
6  
7  
8 (19) Lins, L. ; Thomas-Soumarmon, A. ; Pillot, T. ; Vandekerckhove, J. ; Rosseneu, M. ;  
9  
10 Brasseur, R. *J. Neurochem.* **1999**, *73*, 758-769.  
11  
12 (20) Brasseur, R.: In: *Molecular description of biological components by computer aided*  
13 *conformational analysis*; Brasseur, R., Ed.; CRC Press, Boca Raton, 1990, Vol. 1, p. 203-  
14  
15 219.  
16  
17  
18 (21) Lins, L.; Brasseur R. *FASEB J.* **1995**, *9*, 535-540.  
19  
20 (22) Razafindralambo, H. ; Richel, A. ; Wathelet, B. ; Blecker, C. ; Wathelet, J.P. ; Brasseur,  
21  
22 R. ; Lins, L. ; Miñones Jr., J. ; Paquot, M. *Phys. Chem. Chem. Phys.* **2011**, *13*, 15291-15298.  
23  
24 (23) Razafindralambo, H. ; Blecker, C. ; Mezdour, S. ; Deroanne, C. ; Crowet, J.M. ;  
25  
26 Brasseur, R. ; Lins, L. ; Paquot, M. *J. Phys. Chem. B.* **2009**, *113*, 8872-8877.  
27  
28 (24) Santos, H.A.; Manzanares, J.A.; Murtomäki, L.; Kontturi, K. *Eur. J. Pharm. Sci.* **2007**,  
29  
30 *32*, 105-114.  
31  
32 (25) Marcotte, L. ; Barbeau, J. ; Edwards, K. ; Karlsson, G. ; Lafleur, M. *Colloids Surf. A.*  
33  
34 **2005**, *266*, 51-61.  
35  
36 (26) Tsao, H.-K.; Tseng, W.L. *J. Chem. Phys.* **2001**, *115*, 8125-8132  
37  
38 (27) Bouchemal, K.; Agnely, F.; Koffi, A.; Ponchel, G. *J. Colloid Interface Sci.* **2009**, *338*,  
39  
40 169-176.  
41  
42 (28) Haq, I.; Ladbury, J.E.; Chowdhry, B.Z.; Jenkins, T.C.; Chaires, J.B. *J. Mol. Biol.* **1997**,  
43  
44 *271*, 244-257.  
45  
46 (29) Sinn, C.G.; Dimova, R.; Antonietti, M. *Macromolecules.* **2004**, *37*, 3444-3450.  
47  
48 (30) Goñi, F. M. ; Alonso, A. ; Bagatolli, L. A.; Brown, R. E.; Marsh, D.; Prieto, M.,  
49  
50 Thewalt, J. L. *Biochim. Biophys. Acta.* **2008**, *1781*, 665-684.  
51  
52 (31) Goñi, F. M. ; Alonso, A. *Biochim. Biophys. Acta.* **2009**, *1788*, 169-177.  
53  
54  
55  
56  
57  
58  
59  
60

- 1  
2  
3 (32) Almeida, P.F.F. *Biochim. Biophys. Acta B.* **2009**, 1788, 72-85.  
4  
5  
6 (33) Marsh, D. *Biochim. Biophys. Acta.* **1996**, 1286, 183–223.  
7  
8 (34) Maget-Dana, R. *Biochim. Biophys. Acta.* **1999**, 1462, 109-140.  
9  
10 (35) Deleu, M.; Paquot, M.; Nylander, T. *Biophys. J.* **2008**, 94, 2667-2679.  
11  
12 (36) Demel, R. A.; Geurts Van Kessel, W. S. M.; Zwaal, R. F. A.; Roefofsen, B. *Biochim.*  
13 *Biophys. Acta.* **1975**, 406, 97–107.  
14  
15 (37) Boury, F.; Gautier, J.-C.; Bouligand, Y.; Proust, J.-E. *Colloids Surf. B.* **2001**, 20, 219-  
16 227.  
17  
18 (38) Matti, V.; Säily, J.; Ryhänen, S.J.; Holopainen, J.M.; Borocci, S.; Mancini, G.;  
19 Kinnunen, P.K.J. *Biophys. J.* **2001**, 81, 2135-2143.  
20  
21 (39) Georgiev, G.A.; Kutsarova, E.; Jordanova, A.; Krastev, R.; Lalchev, Z. *Colloids Surf.*  
22 *B.* **2010**, 78, 317-327.  
23  
24 (40) Kanintronkul, Y.; Sriksirin, T.; Angsuthanasombat, C.; Kerdcharoen, T. *Arch.*  
25 *Biochem. Biophys.* **2005**, 442, 180-186.  
26  
27 (41) Kodama, M.; Shibata, O.; Nakamura, S.; Lee, S.; Sugihara, G. *Colloids Surf. B.* **2004**,  
28 33, 211-226.  
29  
30 (42) Eeman, M.; Francius, G.; Dufrière, Y.F.; Nott, K.; Paquot, M.; Deleu M.  
31 *Langmuir.* **2009**, 25, 3029-3039.  
32  
33 (43) Goodrich, F.C.: In: *Proceedings of Second International Congress on Interface*  
34 *Activity*; Schulman, J.H., Ed.; Butterworths/Academic Press, London/New York, 1956, Vol.  
35 1, p. 85.  
36  
37 (44) Hąc-Wydro, K.; Wydro, P.; Dynarowicz-Łątka, P. *J. Colloid Interface Sci.* **2005**, 286,  
38 504-510.  
39  
40 (45) Wydro, P.; Paluch, M. *Colloids Surfaces A.* **2009**, 348, 70-75.  
41  
42  
43  
44  
45  
46  
47  
48  
49  
50  
51  
52  
53  
54  
55  
56  
57  
58  
59  
60

- 1  
2  
3 (46) Eeman, M.; Deleu, M.; Paquot, M.; Thonart, P.; Dufrêne, Y.F. *Langmuir*. **2005**, *21*,  
4  
5 2505-2511.  
6  
7  
8 (47) Shaikh, S.R.; Dumauval, A.C.; Jensi, L.J.; Stillwell, W. *Biochim. Biophys. Acta B*.  
9  
10 **2001**, *1512*, 317-328.  
11  
12 (48) Sun, Y.-T.; Sui, S.-F. *Colloids Surf. A*. **2002**, *198-200*, 239-247.  
13  
14  
15 (49) Rakotomanga, M. ; Loiseau, P.M. ; Saint-Pierre-Chazalet, M. *Biochim. Biophys. Acta*  
16  
17 *B*. **2004**, *1661*, 212-218.  
18  
19 (50) Ishitsuka, Y.; Pham, D.S.; Waring, A.J.; Lehrer, R.I.; Lee, K.Y.C. *Biochim. Biophys.*  
20  
21 *Acta B*. **2006**, *1758*, 1450-1460.  
22  
23  
24 (51) Hąc-Wydro, K.; Jędrzejek, K.; Dynarowicz-Łątka, P. *Colloids Surfaces B*. **2009**, *72*,  
25  
26 101-111.  
27  
28 (52) Subbaiah, P.V.; Sircar, D.; Lankalapalli, R.S.; Bittman, R. *Arch. Biochem. Biophys.*  
29  
30 **2009**, *481*, 72-79.  
31  
32  
33 (53) Kupiainen, M.; Falck, E.; Ollila, S.; Niemela, P.; Gurtovenko, A.A.; Hyvonen, M.T.;  
34  
35 Patra, M.; Karttunen, M.; Vattulainen, I. *J. Comput. Theor. Nanosci*. **2005**, *2*, 401-413.  
36  
37 (54) Slotte, P. J. *Chem. Phys. Lipids*. **1999**, *102*, 13-27  
38  
39 (55) Bouffioux, O.; Berquand, A.; Eeman, M.; Paquot, M.; Dufrêne, Y.F.; Brasseur, R.;  
40  
41 Deleu M. *Biochim. Biophys. Acta*. **2007**, *1768*, 1758-1768.  
42  
43  
44  
45  
46  
47  
48  
49  
50  
51  
52  
53  
54  
55  
56  
57  
58  
59  
60

## Caption legends

Figure 1: Chemical structure of (a) the hexadecylbetainate chloride ( $C_{16}BC$ ) and of the three model lipids selected: (b) Sphingomyelin (SM), (c) palmitoyl-oleoyl-phosphatidylcholine (POPC), and (d) cholesterol (CHOL).

Figure 2: (a) Typical raw data of an ITC experiment. The peaks are related to the successive injections of  $5\mu\text{l}$  of SM/CHOL LUV suspension at  $1000\mu\text{M}$  into a  $30\mu\text{M}$  solution of  $C_{16}BC$  at  $25^\circ\text{C}$ . (b) The cumulative heats of binding ( $\sum\delta h_i$ ) as a function of the lipid concentration in the cell ( $C_L^0$ ). (■) SM/CHOL, ( $\Delta$ ) SM, ( $\blacktriangledown$ ) POPC. The solid line represents the best fit using the Eq 1. The buffer used was PBS at pH 7.4. Error bars are based on reproducibility over at least two independent measurements.

Figure 3: Particle size distribution prior to (full line) and after (dashed line) ITC experiments (a) POPC, (b) SM, (c) SM/CHOL. Inset: value of the mean hydrodynamic diameter ( $d_h$ ) (average of three independent measurements).

Figure 4: Typical adsorption kinetic of  $C_{16}BC$  at a clean air-water interface (○) or into lipid monolayers spread at  $20\text{ mN/m}$ : (■) CHOL, ( $\Delta$ ) SM, ( $\blacktriangledown$ ) POPC. The arrow indicates the moment at which injection occurred.  $C_{16}BC$  is injected at a final concentration of  $1.18\mu\text{M}$  into the subphase (PBS pH 7.4;  $25^\circ\text{C}$ ).

Figure 5: Surface pressure increase ( $\Delta\Pi$ ) caused by the penetration of hexadecylbetainate chloride ( $C_{16}BC$ ) into pure monolayers of (■) CHOL, ( $\Delta$ ) SM, ( $\blacktriangledown$ ) POPC as a function of

1  
2  
3 their initial surface pressure ( $\Pi_i$ ).  $C_{16}BC$  is injected beneath the lipid monolayer at a final  
4 concentration of  $1.18 \mu\text{M}$  in the PBS subphase at pH 7.4 and  $25^\circ\text{C}$ . Error bars are smaller  
5 than symbols in some cases. The solid line represents the linear fitting of the data ( $R^2 = 0.98$   
6 and  $0.99$  for CHOL and SM respectively. For POPC, the linear fitting has been done for  $\Pi_i$   
7  $\geq 10 \text{ mN/m}$  and  $R^2 = 0.98$  ).

8  
9  
10  
11  
12  
13  
14  
15  
16  
17  
18 Figure 6: Surface pressure ( $\Pi$ )–molecular area ( $A$ ) isotherms for  $C_{16}BC$  and lipid mixtures  
19 spread onto PBS subphase pH 7.4 at  $25^\circ\text{C}$ :  $C_{16}BC/POPC$  (a),  $C_{16}BC/SM$  (b) and  
20  
21  
22  
23  
24  
25  
26  
27  
28  
29  
30  
31  
32  
33  
34  
35  
36  
37  
38  
39  
40  
41  
42  
43  
44  
45  
46  
47  
48  
49  
50  
51  
52  
53  
54  
55  
56  
57  
58  
59  
60  
 $C_{16}BC/CHOL$  (c).

Figure 7: Mean molecular area ( $A$ ) versus composition plot for the mixtures of  $C_{16}BC$  with  
POPC (a), SM (b) and CHOL (c) at different  $\Pi$  ( $\Delta$ )  $10 \text{ mN/m}$ , ( $\blacktriangledown$ )  $20 \text{ mN/m}$  and ( $\blacksquare$ )  $30$   
 $\text{mN/m}$  at  $25^\circ\text{C}$ . Straight lines correspond to the ideal mixing behavior (Eq. 3). In some  
cases, the error bars are smaller than the symbols.

Figure 8: Excess free energy of mixing ( $G^{\text{ex}}$ ) and total free energy of mixing ( $G^{\text{M}}$ ) versus  
 $C_{16}BC$  molar ratio for the mixtures of  $C_{16}BC$  with POPC (a, d), SM (b, e) and CHOL (c, f)  
at different  $\Pi$  ( $\Delta$ )  $10 \text{ mN/m}$ , ( $\blacktriangledown$ )  $20 \text{ mN/m}$  and ( $\blacksquare$ )  $30 \text{ mN/m}$  and at  $25^\circ\text{C}$ . Error bars are  
smaller than symbols in some cases.

Figure 9: Total energy of interaction between the pure lipid molecules and between each  
lipid and  $C_{16}BC$ . Black and grey bars correspond to the polar and the hydrophobic  
contributions, respectively.

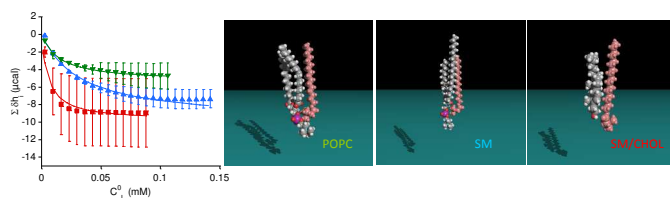
1  
2  
3 Figure 10: Molecular assembly of C<sub>16</sub>BC (in pink) with (a) POPC, (b) SM and (c) CHOL at  
4 an hydrophobic/hydrophilic interface.  
5  
6  
7  
8  
9  
10  
11  
12  
13  
14  
15  
16  
17  
18  
19  
20  
21  
22  
23  
24  
25  
26  
27  
28  
29  
30  
31  
32  
33  
34  
35  
36  
37  
38  
39  
40  
41  
42  
43  
44  
45  
46  
47  
48  
49  
50  
51  
52  
53  
54  
55  
56  
57  
58  
59  
60



1  
2  
3 **Legend of Table**  
4  
5  
6  
7

8 Table 1: Thermodynamic parameters for the binding of C<sub>16</sub>BC to LUV with different  
9  
10 compositions at 25°C  
11  
12  
13  
14  
15  
16  
17  
18  
19  
20  
21  
22  
23  
24  
25  
26  
27  
28  
29  
30  
31  
32  
33  
34  
35  
36  
37  
38  
39  
40  
41  
42  
43  
44  
45  
46  
47  
48  
49  
50  
51  
52  
53  
54  
55  
56  
57  
58  
59  
60

Table of contents Graphic – Table of contents only



Nsimba et al. (revised)